Distributions and averages of electron density parameters: Explaining the effects of gradient corrections

Aleš Zupan
Department of Physical and Organic Chemistry, Jožef Stefan Institute, Jamova 39, 1000 Ljubljana, Slovenia

Kieron Burke
Department of Chemistry, Rutgers University, Camden, New Jersey 08102

Matthias Ernzerhof and John P. Perdew
Department of Physics and Quantum Theory Group, Tulane University, New Orleans, Louisiana 70118

(Received 27 November 1996; accepted 21 March 1997)

We analyze the electron densities $n(\mathbf{r})$ of atoms, molecules, solids, and surfaces. The distributions of values of the Seitz radius $r_s=(3/4\pi n)^{1/3}$ and the reduced density gradient $s=|\nabla n|/(2(3\pi^2)^{1/3}n^{4/3})$ in an electron density indicate which ranges of these variables are significant for physical processes. We also define energy-weighted averages of these variables, $\langle r_s\rangle$ and $\langle s\rangle$, from which local spin density (LSD) and generalized gradient approximation (GGA) exchange-correlation energies may be estimated. The changes in these averages upon rearrangement of the nuclei (atomization of molecules or solids, stretching of bond lengths or lattice parameters, change of crystal structure, etc.) are used to explain why GGA corrects LSD in the way it does. A thermodynamic-like inequality (essentially $d\langle s\rangle/\langle s\rangle > d\langle r_s\rangle/2\langle r_s\rangle$) determines whether the gradient corrections drive a process forward. We use this analysis to explain why gradient corrections usually stretch bonds (but not for example H–H bonds), reduce atomization and surface energies, and raise energy barriers to formation at transition states. © *1997 American Institute of Physics.* [S0021-9606(97)02524-5]

I. INTRODUCTION

Density functional theory (DFT) has become a standard computational tool to calculate the electronic ground state of a system.[1–4] The theory is formally exact,[5] and the only part that needs to be approximated is the exchange-correlation energy[6] as a functional of the spin densities, $E_{\rm xc}[n_\uparrow,n_\downarrow]$. Neglecting small contributions due to the gradient $\nabla\zeta$ of the relative spin polarization, the local spin density (LSD) and generalized gradient (GGA) approximations for $E_{\rm xc}[n_\uparrow,n_\downarrow]$ can be cast in the following form:

$$E_{\rm xc}[n_\uparrow,n_\downarrow]=\int d\mathbf{r}\, n(\mathbf{r})\varepsilon_{\rm x}(r_s(\mathbf{r}))F_{\rm xc}(r_s(\mathbf{r}),\zeta(\mathbf{r}),s(\mathbf{r})), \tag{1}$$

where $n_\uparrow$ denotes the electron density of spin-up electrons, $n_\downarrow$ the electron density of spin-down electrons, and the total density is $n=n_\uparrow+n_\downarrow$. Here $\varepsilon_{\rm x}(r_s)=-(3/4\pi)(9\pi/4)^{1/3}/r_s$ is the exchange energy per electron in the homogeneous electron gas with density $n=(4\pi r_s^3/3)^{-1}$. We use atomic units ($\hbar=e^2=m=1$).

The enhancement factor $F_{\rm xc}(r_s,\zeta,s)$ is a function of three variables: the Seitz radius r_s, the relative spin polarization $\zeta=(n_\uparrow-n_\downarrow)/n$, and the reduced density gradient $s=|\nabla n|/2k_Fn=(3/2\pi)^{1/3}|\nabla r_s|$, where $k_F=(3\pi^2n)^{1/3}$. This factor defines the form and the level of the approximation for the exchange-correlation energy. It can be conveniently split into exchange and correlation parts:

$$F_{\rm xc}(r_s,\zeta,s)=F_{\rm x}(\zeta,s)+F_{\rm c}(r_s,\zeta,s), \tag{2}$$

and the way the variables r_s, ζ, and s are included in the enhancement factor determines the level of approximation:

$$F_{\rm x}(0,0)=1\rightarrow \text{LDA exchange}, \tag{3a}$$

$$F_{\rm x}(\zeta,0)\rightarrow \text{LSD exchange}, \tag{3b}$$

$$F_{\rm x}(\zeta,s)\rightarrow \text{GGA exchange}, \tag{3c}$$

$$F_{\rm c}(r_s,0,0)\rightarrow \text{LDA correlation}, \tag{3d}$$

$$F_{\rm c}(r_s,\zeta,0)\rightarrow \text{LSD correlation}, \tag{3e}$$

$$F_{\rm c}(r_s,\zeta,s)\rightarrow \text{GGA correlation}. \tag{3f}$$

A detailed discussion and analysis of different approximations for $F_{\rm xc}(r_s,\zeta,s)$ can be found in Ref. 7. Fig. 1 shows $F_{\rm xc}(r_s,\zeta,s)$ for the Perdew-Burke-Ernzerhof (PBE) GGA of Ref. 8, an accurate nonempirical functional in which all parameters other than those in LSD are fundamental constants.

The amount of physical knowledge built into the energy functional and the accuracy of it increase with the increasing number of carefully chosen physical variables. None of the approximations (LDA, LSD, GGA) is expected to be valid for $s>>1$. So it is valuable to know how the values of these variables are distributed in real physical systems, which ranges they span, and how they change under chemical reactions, structural transformations, etc. While the smallness of s is a necessary condition for LSD or GGA validity, it is not sufficient. Besides s, there are other measures of density inhomogeneity, such as the reduced Laplacian $\nabla^2n/(2k_F)^2n$ (which diverges at the nuclear cusp of the density, although s is small there).

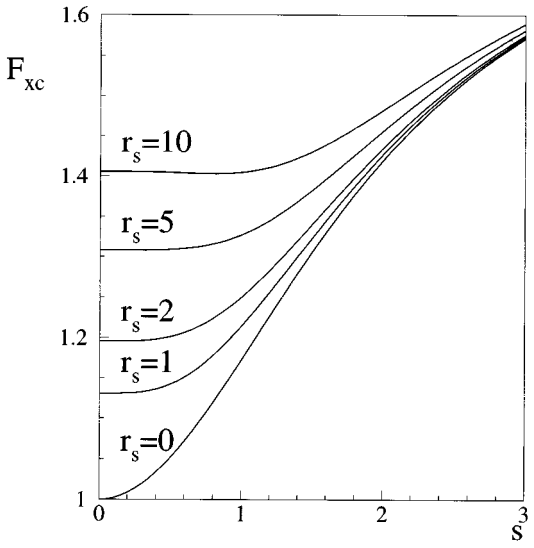

FIG. 1. The enhancement factor $F_{xc}(r_s,\zeta,s)$ of Eq. (1), evaluated for a spin-unpolarized ($\zeta=0$) system in the PBE GGA of Ref. 8, showing the nonlocality or s-dependence.

Neither LSD nor GGA is justified near a nucleus and outside the classical turning surface for the most energetic electron. For two noninteracting electrons bound in the ground state by a Coulomb potential $-Z/r$, this turning surface is a sphere of radius $2/Z$ on which $s=1.43$ and $r_s=2.74/Z$. For this system, $s=0.376\ \exp(2Zr/3)$ and $r_s=(0.721/Z)\ \exp(2Zr/3)$ grow monotonically with r.

Independently of this work, Moll *et al.*[9] have already used the r_s-analysis to explain their LSD and GGA results for the pressure at which Si transforms from the diamond to the β-tin structure. Furthermore, Philipsen and Baerends[10] have used the s-analysis to investigate the importance of the small-s regime ($s\ll 1$) for GGA energies of solids. Ten years ago, Taut[11] defined a ''density spectrum'' related to our r_s-analysis.

The energy of a system depends upon the underlying distributions of the variables r_s, ζ, and s. In earlier work,[12] we proposed a method for calculating the distribution of these variables for atoms and ions. Here we apply that method to calculate distributions for molecules and solids. Then, analogous to the transition from statistical mechanics to thermodynamics, we replace these distributions by carefully-chosen averages. These averages constitute thermodynamic-like variables which fix E_{xc}. We present an inequality which determines whether gradient corrections drive a process forward. The examples we consider include bond-stretching and atomization processes, surface energies and the energy barrier to a chemical reaction.

II. DEFINITIONS

A. Distribution functions defined

To analyze any electronic system, we define distribution functions for two of the constituting variables of the present density functionals:

$$g_1(r_s)=\int d\mathbf{r}\, n(\mathbf{r})\,\delta(r_s-r_s(\mathbf{r})), \tag{4a}$$

$$g_3(s)=\int d\mathbf{r}\, n(\mathbf{r})\,\delta(s-s(\mathbf{r})). \tag{4b}$$

The distribution function $g_2(\zeta)$ for the relative spin polarization ζ is not displayed explicitly in our work, since $\zeta=0$ in many real systems.

The functions $g_1(r_s)$ and $g_3(s)$ have a simple physical interpretation: $g_1(r_s)dr_s$ is the number of electrons in the system with Seitz radius between r_s and r_s+dr_s, while $g_3(s)ds$ is the number of electrons in the system with reduced density gradient between s and $s+ds$. Thus they are analogs of the density of states for energy levels. They are normalized to N, the number of electrons in the system:

$$\int_0^\infty dr_s g_1(r_s)=\int_0^\infty ds g_3(s)=N. \tag{5}$$

A detailed description of the numerical method by which they are evaluated was given elsewhere.[12]

B. Averages defined

The method of the previous subsection yields information about *all* values of the variable being analyzed. In this section, we define average values of r_s, ζ, and s for any electronic system, which summarize (roughly) the information contained in the distribution functions.

The energy-weighted averages $\langle r_s\rangle$, $\langle|\zeta|\rangle$, and $\langle s\rangle$ are defined by:

$$\varepsilon_x(\langle r_s\rangle)=\frac{\int d\mathbf{r}\, n\varepsilon_x(r_s)}{\int d\mathbf{r}\, n}=\frac{E_x^{\mathrm{LSD}}[n/2,n/2]}{N}, \tag{6a}$$

$$F_x(\langle|\zeta|\rangle,0)=\frac{\int d\mathbf{r}\, n\varepsilon_x(r_s)F_x(\zeta,0)}{\int d\mathbf{r}\, n\varepsilon_x(r_s)}=\frac{E_x^{\mathrm{LSD}}[n_\uparrow,n_\downarrow]}{E_x^{\mathrm{LSD}}[n/2,n/2]}, \tag{6b}$$

$$F_x(0,\langle s\rangle)=\frac{\int d\mathbf{r}\, n\varepsilon_x(r_s)F_x(0,s)}{\int d\mathbf{r}\, n\varepsilon_x(r_s)}=\frac{E_x^{\mathrm{GGA}}[n/2,n/2]}{E_x^{\mathrm{LSD}}[n/2,n/2]}. \tag{6c}$$

Note that only the exchange part of the exchange-correlation energy is used to define the average values of r_s, ζ, and s. Because we average only monotonic functions of one *variable* at a time, our $\langle x\rangle$ (where $x=r_s,\zeta$, or s) is a true average, falling between the minimum and maximum values of x present in our system. If unpolarized exchange dominates other effects, or if the distribution of each variable is not too broad, these averages can be used to estimate E_{xc}.

This idea can be tested as follows. Write

$$E_{xc}^{\mathrm{LSD}}[n_\uparrow,n_\downarrow]=R_{xc}^{\mathrm{LSD}}N\varepsilon_x(\langle r_s\rangle)F_{xc}(\langle r_s\rangle,\langle|\zeta|\rangle,0), \tag{7a}$$

$$E_{xc}^{\mathrm{GGA}}[n_\uparrow,n_\downarrow]=R_{xc}^{\mathrm{GGA}}N\varepsilon_x(\langle r_s\rangle)F_{xc}(\langle r_s\rangle,\langle|\zeta|\rangle,\langle s\rangle). \tag{7b}$$

If the ratios R_{xc}^{LSD} and R_{xc}^{GGA} are close to one (as indeed they typically are), then the averages defined in Eqs. (6) can be used to estimate either the LSD or GGA exchange-correlation energy of the system, using Eqs. (7) with R_{xc}^{LSD} and R_{xc}^{GGA} set equal to 1.

Although the corresponding relative errors of exchange-correlation energy differences *are* often larger than those of E_{xc} itself, they are still small enough for purposes of the qualitative analysis we shall make in Section III B.

The numerical method to calculate the average values is straightforward to implement. Once the LSD and GGA energies on the right-most side of the definition (6) have been calculated for a system, the average values of the density variables are found as the roots of the equations.

C. Uniform scaling behavior

To illustrate the definitions and for later use in Section III B 2, we consider uniform scaling. Uniform density scaling $n(\mathbf{r}) \rightarrow \gamma^3 n(\gamma \mathbf{r})$ by a parameter γ leaves the electron number N unchanged, but transforms $r_s(\mathbf{r})$ to $r_s(\gamma \mathbf{r})/\gamma$, $\zeta(\mathbf{r})$ to $\zeta(\gamma \mathbf{r})$, and $s(\mathbf{r})$ to $s(\gamma \mathbf{r})$. Under this transformation, $g_1(r_s)$ and $\langle r_s \rangle$ transform to $\gamma g_1(\gamma r_s)$ and $\langle r_s \rangle/\gamma$, respectively, while $g_3(s)$, $\langle |\zeta| \rangle$, and $\langle s \rangle$ remain invariant.

III. RESULTS AND DISCUSSION

We performed both analyses on a set of systems, including atoms and simple diatomic molecules, transition-state molecular structures, and different crystal phases of covalent and ionic crystals. The Hartree–Fock electronic densities for all the treated systems were calculated with the CRYSTAL 92 program,[13,14] an *ab initio* Gaussian-type-basis LCAO program, that can treat electronic systems extended in 0 (atoms, molecules), 1 (polymers), 2 (surfaces), and 3 (crystals) dimensions. Detailed description of the method can be found in Ref. 15. A DFT extension of the CRYSTAL program[16] was used to compute the integrals in Eq. (4) and to evaluate the DFT exchange-correlation energies needed in Eqs. (6). In the present work we use the PBE[8] (Perdew–Burke–Ernzerhof) form of the enhancement factor, a simplified version of the PW91 GGA for the exchange-correlation energy functional.[17–19]

As an alternative to the Hartree–Fock densities, we could have used self-consistent LSD or GGA densities. However, the typical differences between GGA and LSD are found whether or not the GGA is implemented self-consistently. We tested this claim numerically for the N_2 molecule. First we calculated the Hartree–Fock, LSD, and GGA densities self-consistently at the experimental bond length. Then we also optimized the bond length in each approximation. Differences were no more than 0.003 for $\langle r_s \rangle$ and 0.002 for $\langle s \rangle$.

To avoid basis-set error we used a rich 6-311++$G(3df,3pd)$ basis set[20] for H, Li, N, and Ar atoms. For computational expediency in Si and LiF crystals we used smaller basis sets optimized for calculations in solids. (See Ref. 21 for Si and Ref. 22 for LiF crystal.)

To calculate the exchange-correlation energies E_{xc} in equations (6) we used the maximum standard level of accuracy defined in the CRYSTAL DFT extension.[16] At this level of accuracy (30 000 reducible points per atom) the average relative error in exchange-correlation energy is $3 \cdot 10^{-6}$. To calculate the functions in equations (4) we used a very fine integration grid with approximately 100 000 reducible points per atom.

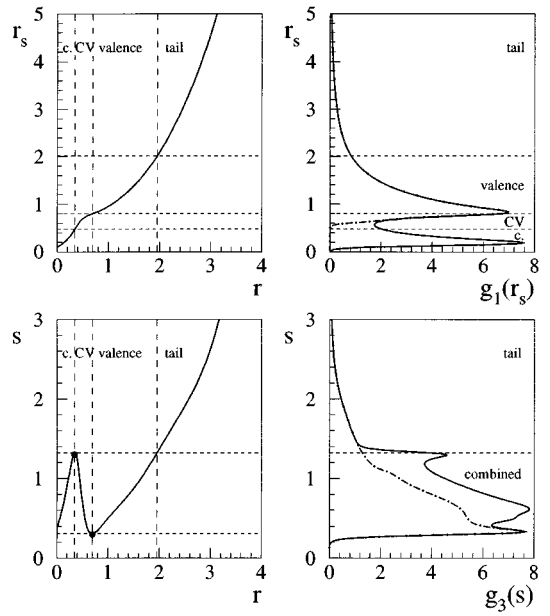

FIG. 2. Four-panel plot of density variables and their distributions for the N atom. The left two panels present $r_s(r)$ and $s(r)$, where r is the radial distance in bohr from the center of the atom. The right two panels present the corresponding $g_1(r_s)$ and $g_3(s)$ distribution functions. The number of electrons in each region is: core (c.) 1.77, core-valence overlap (CV) 0.88, valence 3.45, and tail 0.90. The dash-dot line plots the distribution functions without the contribution of the 2 electrons from the core.

A. Distribution functions evaluated

The calculation of distribution functions yields much information about a given variable. Some examples for atoms and ions have appeared elsewhere.[12] Here we extend the analysis to include the N atom, the N_2 molecule, and bulk Si.

In Fig. 2 we show a four-panel plot for the N atom. The key plot is the bottom-left one where the reduced density gradient s is plotted as a function of the radial distance r (in bohr), starting from the atomic center. Note how sensitive the reduced density gradient s is to the shell structure of the atom. We may easily distinguish the shell regions in real space, where s is monotonically rising, and inter-shell regions, where s is monotonically falling. We identify four regions of interest.[12] The core region extends from $r=0$ to the outermost maximum of s. The pure valence region extends from the outermost minimum of s to the point where $s(r)$ attains the same value as the maximum value of s in the core region. Thus the valence electrons have reduced density gradients no larger than those in the core. Between the core and the valence region, where s is falling monotonically, is the mixed core-valence (CV) overlap region. The remaining region, where s is bigger then any s in the core and is exponentially and monotonically rising up to infinity, is called the tail region, which is defined to clarify our later discussion of $g_3(s)$ figures.

These regions in real space can also be marked on the upper-left panel, where r_s is depicted as a function of the

radial distance r. The curve $r_s(r)$ is monotonic and therefore regions in real space uniquely map to regions in r_s space. The partitioning in r_s space is transferred to the upper-right plot, where the density function $g_1(r_s)$ is plotted sideways. The shell structure is prominent. There is one peak for each full or partially filled shell. The core electron peak is at $r_s \approx 0.20$, the valence peak at $r_s \approx 0.83$.

The $s(r)$ curve at the lower left plot is not monotonic, so we cannot partition the density function $g_3(s)$ in the lower right plot into four simple regions. In fact only two regions can be separated: a combined one, that comprises of core and valence electrons, and a tail region. In this case, we can still eliminate core contributions simply by excluding any contribution from $r \leqslant r_c$ in the integration of Eq. (4), where r_c is defined to include the integer number of electrons in the core. For the N atom, there are 2 electrons in the core, and r_c is about 0.43 bohr. The resulting valence-only distribution functions are marked as dash-dot lines in the figures, and separate the core and valence contributions in $g_3(s)$.

The four-panel plot in Fig. 2 shows which values of r_s and s contribute significantly to integrals over the density. Only 1/10th of an electron has $r_s > 5.52$, and only 1/10th has $s > 3.24$. Such values for r_s vary from atom to atom, but $g_3(s)$ always falls abruptly at the border between the combined and tail regions, and the significant contribution very rarely extends above the value of $s = 3$.

Next we consider the change in distribution due to the atomization of the N_2 molecule. In Fig. 3, we plot the difference of the distributions between the two isolated atoms and the molecule. In the $\Delta g_1(r_s)$ plot we observe a shift of electrons from smaller to larger r_s values. This reflects the fact that the density expands during atomization. The net charge shifted (area of the first negative peak) is 0.9 electrons. The core electrons remain largely unaffected, since the dash-dot core-less line is almost indistinguishable from the solid all-electron line. Now 1/10th of an electron has $r_s > 5.02$ in the contribution to $\Delta g_1(s)$, while 1/10th has $s > 2.55$ in the contribution to $\Delta g_3(s)$.

A look at the lower panel for $\Delta g_3(s)$ shows that, upon atomization, there is a shift of electrons from lower to higher values of the reduced gradient s. (The area of the first negative peak is 1.1 electrons.) This can be understood as follows: In the tail of an isolated atom, the reduced density gradient s goes to infinity. The electrons in the bond between two atoms have smaller reduced gradients which actually vanish right at the bond center. The wriggle at $s \approx 1.3$ is an artifact of the distribution function due to the sharp change in s on passing from the core to the core-valence region. Its net integrated effect is approximately zero. The core-less distribution function $\Delta g_3(s)$ indicated by the dashed-dotted line smoothly ignores this feature.

Figure 4 shows the derivative of the distribution functions with respect to the bond length or lattice constant a evaluated at the experimental value $(adg/da|_{a=a_0})$. The similarity between Figs. 3 and 4 is obvious and natural. Note, however, that the large-s contribution of Fig. 3 is suppressed in Fig. 4.

In Fig. 5 we plot the distribution functions for silicon crystalized in a tetragonal diamond structure, using the experimental value for the lattice parameter 5.43 Å.[23] The plots depict the same qualitative behavior as those for atoms and molecules. The chief difference can be seen in the tails of the distributions, where they fall exactly to zero (at $r_s = 4.8$ and at $s = 1.9$). In an infinite periodic system, the density never vanishes, and the reduced gradient never goes to infinity.

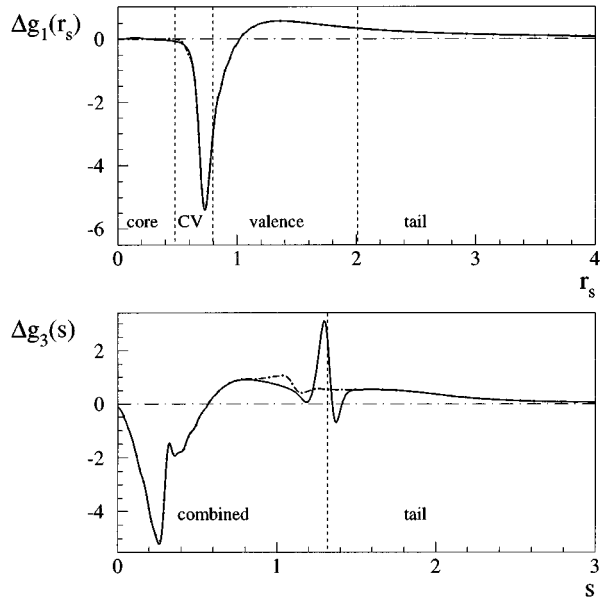

FIG. 3. Change of the distribution functions upon atomization of the N_2 molecule. In the upper plot, 0.9 of an electron is shifted; in the lower plot, 1.1 is shifted. The ''regions'' shown here and in Figs. 4 and 5 are those for the isolated atom.

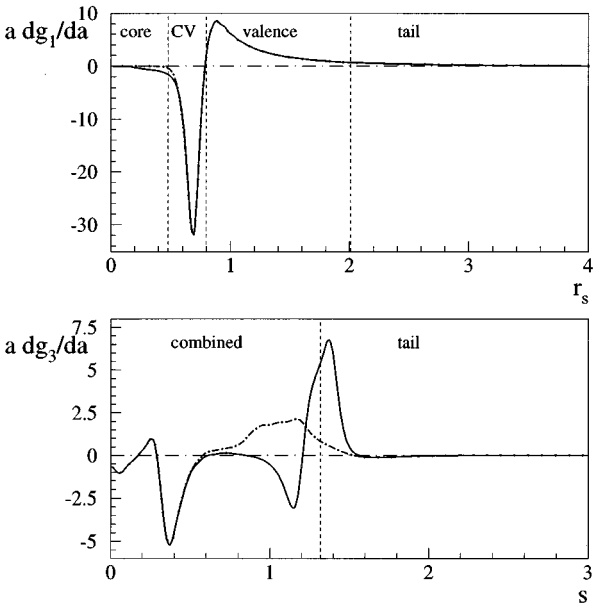

FIG. 4. The derivative with respect to bond length a of the distribution functions $g_1(r_s)$ and $g_3(s)$ for the N_2 molecule at its experimental bond length.

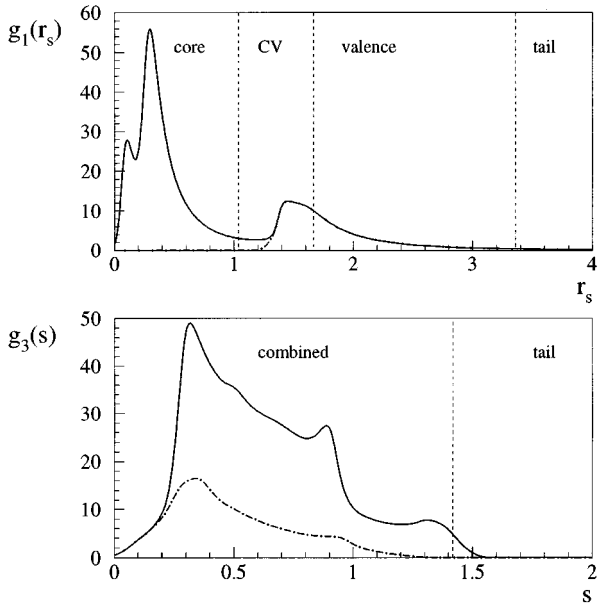

FIG. 5. $g_1(r_s)$ and $g_3(s)$ distribution functions for bulk Si in the diamond structure at the experimental lattice parameter.

The range of s that contributes to $g_3(s)$ and $\Delta g_3(s)$ coincides with that for which the GGA is expected to be valid. This is especially so in the solid state.

B. Average values evaluated

1. Interpretation and behavior

The average value of the reduced density gradient $\langle s \rangle$ of Eq. (6c) is a measure of the inhomogeneity of the system. For a homogeneous electron gas its value is exactly zero, and it increases with increasing departure of the electron density from the homogeneous limit. So we expect that $\langle s \rangle$ increases when we atomize a molecule or solid, stretch a molecular bond or lattice constant, or distort a solid to a more open crystal structure.

We tested this expectation on a set of test cases. The results are presented in Tables I and II. We used experimental bond lengths for the molecules[24] and bulk Si.[23] For LiF in the fcc phase, in which it exists under normal conditions, we use the experimental value.[23] We choose the lattice parameter of the high-pressure bcc phase so that the volume per formula unit is the same for fcc and bcc phases.

The right-most columns with the values of R_{xc}^{LSD} and R_{xc}^{GGA} in Table I confirm that the definition of the averages (6) is a useful one, since all values are close to one. R_{xc}^{GGA} is somewhat closer to 1 than is R_{xc}^{LSD}, reflecting the suppression of correlation relative to exchange that occurs as we pass from LSD to GGA. Our expectation is confirmed: $\langle s \rangle$ increases when going from a molecule or solid to its separated atoms, and from a shorter bond length to a longer one. (The quantity $ad\langle s \rangle/da|_{a=a_0}$ in Table II is always positive.)

TABLE II. Derivatives of the average quantities with respect to the bond length, evaluated at the experimental bond length.

System	$\frac{ad\langle r_s \rangle}{da}$	$\frac{ad\langle \lvert\zeta\rvert \rangle}{da}$	$\frac{ad\langle s \rangle}{da}$
H_2	0.624	0.000	0.026
H_3	0.680	0.109	0.095
Li_2	0.033	0.000	0.014
N_2	0.067	0.000	0.064
LiF (mol)	0.012	0.000	0.021
LiF (fcc)	0.031	0.000	0.070
LiF (bcc)	small	0.000	small
Si (diamond)	0.019	0.000	0.041

2. Understanding gradient corrections

In this section, we use the averages defined in Section II B to explain the effect of gradient corrections on many

TABLE I. This table summarizes the average values of $\langle r_s \rangle$ (in bohrs), $\langle \lvert\zeta\rvert \rangle$, and $\langle s \rangle$ for all the Hartree–Fock densities we have studied. The second column represents the difference between GGA and LSD exchange-correlation energies (in mH). The R_{xc} values in the two right-most columns are close to 1, satisfying the requirements discussed after Eq. (7). For molecules and solids the average values were calculated at the experimental bond lengths or lattice constants (Refs. 24 and 23) (H_2:0.741 Å, Li_2:2.67 Å, N_2:1.098 Å, LiF (molecule):1.564 Å, LiF (fcc):3.99 Å, LiF (bcc):2.51 Å, bulk Si:5.43 Å).

System	$E_{xc}^{GGA}-E_{xc}^{LSD}$	$\langle r_s \rangle$	$\langle \lvert\zeta\rvert \rangle$	$\langle s \rangle$	R_{xc}^{LSD}	R_{xc}^{GGA}
H	−21.7	2.154	1.000	1.079	0.997	1.007
H_2	−29.3	1.617	0.000	0.885	0.994	1.000
Li^+	−115.3	0.645	0.000	0.895	0.996	0.999
Li	−121.6	0.903	0.241	0.901	0.982	0.992
Li_2	−233.8	0.892	0.000	0.888	0.986	0.996
N	−404.6	0.558	0.343	0.780	0.989	0.999
N_2	−772.0	0.542	0.000	0.747	0.992	1.002
F^-	−551.5	0.489	0.000	0.711	0.992	1.000
LiF (mol)	−662.3	0.507	0.000	0.732	0.993	1.000
$Li^+ + F^-$	−666.8	0.510	0.000	0.736	0.993	1.000
LiF (fcc)	−650.2	0.504	0.000	0.723	0.993	1.000
LiF (bcc)	−653.9	0.504	0.000	0.723	0.993	1.000
Si	−1022.4	0.345	0.100	0.656	0.992	0.999
Si (diamond)	−1997.7	0.341	0.000	0.641	0.993	1.000
Ar	−1413.1	0.296	0.000	0.620	0.993	0.999

properties of systems. Relative to LSD, GGA reduces atomization energies,[18,25–27] usually (but not always) stretches and softens bonds or lattice constants,[18,26,28,29] and favors open crystal structures relative to close-packed ones.[9,30,31] For a set of 20 molecules,[8] the mean errors of the atomization energies are 1.4 eV for LSD and 0.3 eV for the PBE GGA.

To understand the origin of these effects, we consider the difference between the LSD and GGA total energies. Since E^{LSD} is minimal with respect to variations of $n(\mathbf{r})$, we can usually ignore the small differences between self-consistent LSD and GGA densities,[32] so that $E^{\mathrm{GGA}}-E^{\mathrm{LSD}}\approx E_{\mathrm{xc}}^{\mathrm{GGA}}-E_{\mathrm{xc}}^{\mathrm{LSD}}$. We assume that our average values for the density parameters work well (i.e., $R_{\mathrm{xc}}\approx 1$ in Eq. (7)), permitting a kind of thermodynamic analysis. Then the gradient correction to the energy per electron for a given density is:

$$\Delta=(E_{\mathrm{xc}}^{\mathrm{GGA}}-E_{\mathrm{xc}}^{\mathrm{LSD}})/N$$

$$\approx\varepsilon_{\mathrm{x}}(\langle r_s\rangle)[F_{\mathrm{xc}}(\langle r_s\rangle,\langle|\zeta|\rangle,\langle s\rangle)-F_{\mathrm{xc}}(\langle r_s\rangle,\langle|\zeta|\rangle,0)]. \qquad (8)$$

Now consider some infinitesimal process at fixed N (e.g., stretching a bond) which leads to infinitesimal changes in $\langle r_s\rangle$, $\langle|\zeta|\rangle$, and $\langle s\rangle$. The gradient correction to LSD will favor this process if $d\Delta<0$. Since $\partial\Delta/\partial\langle s\rangle<0$, partial differentiation of Eq. (8) yields:

$$\frac{d\langle s\rangle}{\langle s\rangle}>P\frac{d\langle r_s\rangle}{2\langle r_s\rangle}+Qd\langle|\zeta|\rangle, \quad (d\Delta<0), \qquad (9)$$

where

$$P=-\frac{2\langle r_s\rangle}{\langle s\rangle}\frac{\partial\Delta/\partial\langle r_s\rangle}{\partial\Delta/\partial\langle s\rangle}, \qquad (10a)$$

$$Q=-\frac{1}{\langle s\rangle}\frac{\partial\Delta/\partial\langle|\zeta|\rangle}{\partial\Delta/\partial\langle s\rangle}. \qquad (10b)$$

(We choose this normalization of P so that, for $\langle|\xi|\rangle=0$, $P\to 1$ as $\langle r_s\rangle\to 0$ and $\langle s\rangle\to 0$; in this limit, $F_{\mathrm{xc}}\to 1+\mu s^2$ where μ is a positive constant.) Equation (9) shows that, contrary to popular belief, the increase in inhomogeneity ($d\langle s\rangle$) must be greater than some *minimum* value, which can be greater than zero, for gradient corrections to favor a process. If the increase in inhomogeneity is insufficient, the gradient corrections will disfavor the process. (The inequality (9) is an exact condition only when the R_{xc} factors of Eq. (7) are exactly equal to one. Since it is simple to calculate $d\Delta$ directly, the role of this inequality (9) is in any case purely explanatory.)

We plot the gradient contribution to the exchange-correlation energy per electron in Fig. 6. We choose values of r_s and s which cover the range of average values of these variables (appearing in Tables I and V). The correction is larger for larger densities, and depends only weakly on spin polarization. This is due to the form of the enhancement factor F_{xc} plotted in Fig. 1. The factor $P(r_s,\zeta,s)$ is plotted in Fig. 7 and is of order 1, whereas the factor Q is small and can usually be neglected.

As an illustration of Eq. (9), we consider an infinitesimal density contraction ($d\gamma>0$ in Section II C). We find

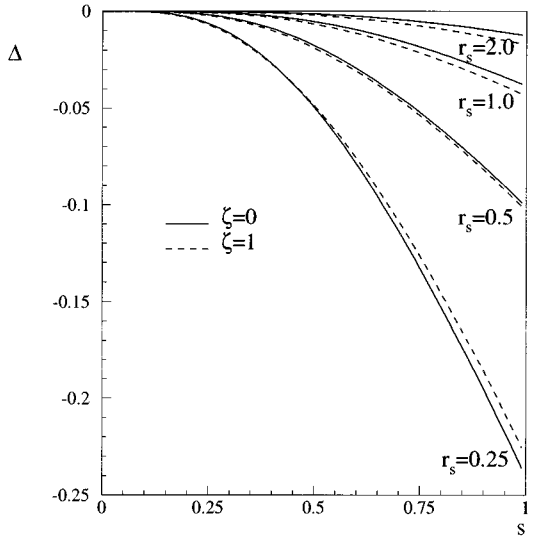

FIG. 6. GGA gradient correction Δ of Eq. (8) (in hartrees) to the exchange-correlation energy per electron for different values of r_s for the unpolarized ($\zeta=0$) and fully polarized ($\zeta=1$) cases, using the PBE functional.

$d\langle s\rangle=d\langle|\zeta|\rangle=0$ while $d\langle r_s\rangle<0$, so the inequality (9) is satisfied and thus this process is driven forward by gradient corrections. Gradient corrections favor density contraction (smaller $\langle r_s\rangle$) as well as density inhomogeneity (greater $\langle s\rangle$), as can be seen directly from Fig. 6. Thus the self-consistent LSD density of N_2 has $\langle r_s\rangle=0.544$ bohr and $\langle s\rangle=0.746$, while the self-consistent GGA density has $\langle r_s\rangle=0.541$ bohr and $\langle s\rangle=0.747$.

3. Bond stretching

Next we apply Eq. (9) to the question of whether GGA stretches bonds relative to LSD. By the argument preceding Eq. (8), $Nd\Delta/da\approx dE^{\mathrm{GGA}}/da$ at the LSD equilibrium bond

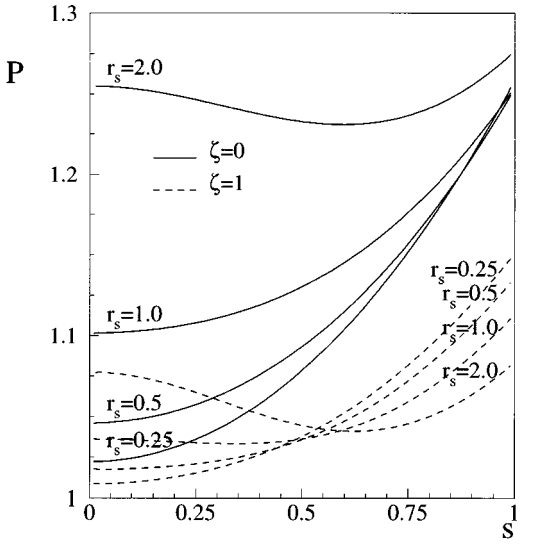

FIG. 7. Function $P(r_s,\zeta,s)$ of Eq. (10a) for different values of r_s for the unpolarized and fully polarized cases, using the PBE functional.

TABLE III. Quantities from Eq. (9) for infinitesimal changes around the experimental bond length. The small changes $d\langle r_s\rangle$, $d\langle|\zeta|\rangle$, $d\langle s\rangle$ were calculated by stretching the bond length by $\pm 1\%$. The inequality (9) is satisfied whenever gradient corrections favor bond stretching.

System	P	Inequality		
H_2	1.23	$5.80\cdot10^{-4}$	$<$	$4.76\cdot10^{-3}$
Li_2	1.21	$3.18\cdot10^{-4}$	$>$	$2.45\cdot10^{-4}$
N_2	1.16	$1.71\cdot10^{-3}$	$>$	$1.43\cdot10^{-3}$
LiF	1.15	$5.19\cdot10^{-4}$	$>$	$2.39\cdot10^{-4}$
Si	1.12	$1.35\cdot10^{-3}$	$>$	$6.33\cdot10^{-4}$
LiF (fcc)	1.15	$2.20\cdot10^{-3}$	$>$	$7.20\cdot10^{-4}$
H_3	1.22	$2.17\cdot10^{-3}$	$<$	$4.62\cdot10^{-3}$

length. If $d\Delta<0$ when a is increased infinitesimally, the bond expands due to gradient corrections, but it contracts if $d\Delta>0$. The average reduced density gradient $\langle s\rangle$ increases with bond length (Table II). But $\langle r_s\rangle$ also increases, since the average density drops as the atoms separate. The inequality (9) is tested for the bond lengths in Table III. Usually the inequality of Eq. (9) is fulfilled, which implies that bond lengths are longer in GGA than in LSD.

However, in a few cases the increase of inhomogeneity is insufficient to overcome the decrease in the density. This holds true for the hydrogen molecule H_2 ($a_0^{\mathrm{LSD}}=0.765$ Å, $a_0^{\mathrm{GGA}}=0.748$ Å, $a_0^{\mathrm{exper.}}=0.741$ Å) and the H_3 molecule at the transition state ($d_{TS}^{\mathrm{LSD}}=0.950$ Å, $d_{TS}^{\mathrm{GGA}}=0.941$ Å). For both these cases, the inequality of Eq. (9) is violated, and indeed GGA shrinks these bonds relative to LSD. The absence of an ionic core in the H atom leads to an unusual degree of density contraction under bond-length shrinkage. As found in Ref. 26, gradient corrections often shrink bonds to H atoms. But they correctly stretch the weak hydrogen bond in ice,[33] where little relative change in $\langle r_s\rangle$ is expected. The GGA improvement over LSD for hydrogen-bonded systems was first shown in Ref. 34.

An alternative explanation of these effects is given in Ref. 35 in terms of the self-consistent effect of the gradient corrections upon the electron density of the atom: The radii of the hydrogen atom and of all 1*s* core states in other atoms contract. The resulting stronger screening of the nuclear attraction then permits an expansion of the radii of the valence orbitals in the other atoms.

Although the effects of gradient corrections on the lattice constants of solids are typically small, they can still have a profound influence upon the equilibrium crystal structure and magnetism.[36,37]

4. Surface energies

As a final example of an infinitesimal process, we apply our analysis to the surface contribution to the exchange-correlation energy of an infinite solid. We consider a jellium slab with an infinite barrier at the surface, for which the density profile can be written analytically. (The overall trends are similar to those for the self-consistent barrier associated with a step edge to the positive background.[18]) We define the surface contribution to the exchange-correlation energy as the difference between the exchange-correlation energy of a piece of the system with a surface and that of a bulk piece containing the same number of electrons, in the limit where the width of the sample becomes infinite. Because the bulk is uniform, in the thermodynamic limit $\langle s\rangle\to 0$ and LSD becomes exact. However, the surface contribution is determined by how $\langle s\rangle\to 0$. We find

$$\langle r_s\rangle\to r_s(1+0.256/L),\quad (L\to\infty) \tag{11}$$

and

$$\langle s\rangle\to O+\frac{\beta(r_s)}{\sqrt{L}},\quad (L\to\infty), \tag{12}$$

where $L=2k_FW_{1/2}$, and $W_{1/2}$ is the half-width of the jellium slab. In the range $0\leqslant r_s\leqslant 6$, we find $1\leqslant D_{\mathrm{xc}}^{\mathrm{LSD}}\leqslant 1.02$, $1\geqslant D_{\mathrm{xc}}^{\mathrm{GGA}}\geqslant 0.89$, and $0\leqslant\beta\leqslant 1.071$, where the D_{xc} are the analogs for energy differences of the ratios R_{xc} defined in Eq. (7). The values of D_{xc} indicate that the surface contribution is (moderately) well-predicted by our averages. Since both $d\langle s\rangle$ and $d\langle r_s\rangle>0$ for creation of a jellium surface, while $\langle s\rangle=0$, our inequality of Eq. (9) is trivially satisfied, so that GGA will always lower the surface exchange-correlation energy relative to LSD. For more realistic surfaces, quantitative evaluation of our inequality is necessary, as $\langle s\rangle\neq 0$ in the bulk. For example, there is a slight reduction in the surface energy of Ag(100) in going from GGA to LSD.[38]

Note also that the $L^{-1/2}$ correction to $\langle s\rangle$ is a peculiarity of a jellium surface, and that β is determined by the small s behavior of F_{x}. For any nonuniform bulk, $\langle s\rangle\to\langle s\rangle_{\mathrm{bulk}}+O(1/L)$, where $\langle s\rangle_{\mathrm{bulk}}$ is the bulk value.

5. Atomization energies

Next we apply Eq. (9) to finite changes. Although we derived this result for infinitesimal changes in average density values, we can apply it to finite changes, assuming those changes are not so large as to render it invalid. In doing so, we replace the infinitesimal changes by finite changes and insert parameter values that are the arithmetic averages of the initial and final state values.

An immediate application is to atomization energies of molecules and solids. The atomization energy, a positive quantity for a stable molecule (or solid), is defined as the difference between the total energy of the separated atoms and that of the molecule (or of the unit cell in the crystal). The total energy includes the exchange-correlation part, which is approximated either by LSD or GGA. It is well known that LSD always overestimates the atomization energy, whereas GGA comes much nearer to the experimental value. (See for example Ref. 27.)

For all systems but the homogeneous electron gas, the GGA approximation lowers the energy relative to LSD (second column in Table I and Fig. 6). The amount of the lowering depends on the average value $\langle s\rangle$, which is smaller for the molecule than for the isolated atoms. Thus atomization energies are lower in GGA.

In Table IV we list values of P and Q for atomization processes. As seen in the right-most column, the inequality (9) is never violated, which means the GGA binding energy

TABLE IV. Quantities from Eq. (9) for atomization processes. Inequality (9) is satisfied whenever gradient corrections lower the atomization energy.

System	P	Q	Inequality		
$H_2 \rightarrow 2H$	1.23	$-5.04\cdot10^{-2}$	$1.98\cdot10^{-1}$	$>$	$1.25\cdot10^{-1}$
$N_2 \rightarrow 2N$	1.16	$1.90\cdot10^{-3}$	$4.32\cdot10^{-2}$	$>$	$1.76\cdot10^{-2}$
$Li_2 \rightarrow 2Li$	1.21	$-1.65\cdot10^{-3}$	$1.45\cdot10^{-2}$	$>$	$7.39\cdot10^{-3}$
$LiF \rightarrow Li^+ + F^-$	1.15	0.00	$6.80\cdot10^{-3}$	$>$	$3.40\cdot10^{-3}$
$Si^{bulk} \rightarrow Si$	1.12	$1.16\cdot10^{-3}$	$2.47\cdot10^{-2}$	$>$	$8.27\cdot10^{-3}$
$LiF^{fcc} \rightarrow Li^+ + F^-$	1.15	0.00	$1.92\cdot10^{-2}$	$>$	$6.81\cdot10^{-3}$
$H_3 \rightarrow H + H_2$	1.22	$-4.09\cdot10^{-2}$	$6.76\cdot10^{-2}$	$>$	$-1.42\cdot10^{-2}$
$HN_2 \rightarrow H + N_2$	1.16	$1.06\cdot10^{-3}$	$1.20\cdot10^{-2}$	$>$	$4.11\cdot10^{-3}$

is lower than the LSD energy for every reaction listed in the table. The inequality is close for H_2, because of the large increase in $\langle r_s \rangle$ that occurs upon atomization of this molecule, and indeed the GGA lowering of the binding energy of H_2 is unusually small in both an absolute and a relative sense.[8]

6. Transition state barriers

Our final example is the energy barrier to formation at a transition state, which is usually underestimated by LSD. In many cases LSD predicts no barrier. GGA gives higher energy barriers which are nearer to experimental values.[39,40] An early explanation[39] focussed on the self-consistent effect of gradient corrections on the density, even though the authors of Ref. 39 found that gradient corrections still raised the barrier when applied non-self-consistently to LSD densities. We present a simpler explanation here, which translates into physical language the chemical explanation of Ref. 40: LSD favors bonds too much, and so lowers the energy of the transition-state complex relative to that of the separated reactants.

We have chosen two simple reactions as test cases: hydrogen transfer in the reaction $H+H_2 \rightarrow H_2+H$, and a hydrogen addition to N_2. The reason to choose these two reactions is their simplicity. Also a sufficient literature is available on this topic (see Refs. 41 and 42 for the $H+H_2 \rightarrow H_2+H$ reaction, and Refs. 43 and 44 for the $H+N_2 \rightarrow HN_2$ reaction).

For the first reaction (hydrogen transfer) we used LSD densities, just as in Ref. 41. The geometry of the transition from one structure to another is linear and the transition state has a very high symmetry ($D_{\infty h}$). We chose one of the bonds to be a reaction coordinate d_{reac}, running from infinity to 0.95 Å, which is the LSD bond length at the transition state. At each value of d_{react} we optimized the second or dependent bond length d_{dep} and then calculated the DFT exchange-correlation energies needed to find the average values of $\langle r_s \rangle$, $\langle |\zeta| \rangle$, and $\langle s \rangle$.

The most important quantity $\langle s \rangle$ in our analysis is plotted in Fig. 8. Its value is highest when the hydrogen atom is far away from the H_2 molecule (d_{react} is big) and minimizes at the transition state. A similar story can be told for the hydrogen addition to N_2. The reaction coordinate is here the distance between the hydrogen and one nitrogen atom. Two dependent coordinates, which are optimized for each value of reaction coordinate, are the N-N distance and the angle H-N-N. Again the average value $\langle s \rangle$ is the highest for a configuration where the H atom is far away from the N_2 molecule, and $\langle s \rangle$ decreases all the way to the equilibrium energy. The value of $\langle s \rangle$ at the transition state is higher than at the equilibrium geometry, but lower than when the parts are separated (Table V).

We can now explain why GGA gives higher energy barriers than LSD does. LSD usually gives a small energy barrier, or none. In fact, H_3 is bound at the LSD level,[41,42] i.e., the LSD total energy is more negative for the TS then for the separate reactants. Gradient corrections lower the energy of the separate reactants (larger $\langle s \rangle$) more than they lower the energy of the TS (smaller $\langle s \rangle$). As Table IV shows, the inequality of Eq. (9) is satisfied by the break-up of the transition state, which is thus favored by gradient corrections.

Our calculations on the LSD densities confirm this expectation. For the $H+H_2$ reaction, the energy barriers in eV are -0.11 in LSD, 0.15 in the PBE GGA, and experimentally 0.42.[45] For the $H+N_2$ reaction, the corresponding barriers to the formation of HN_2 are 0.03 in LSD, and 0.32 in

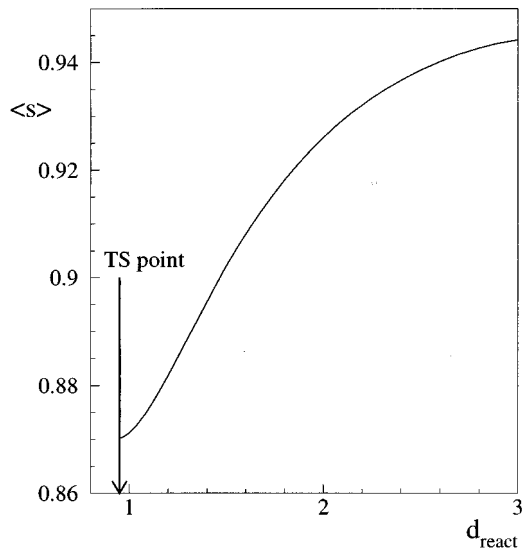

FIG. 8. The average reduced density gradient $\langle s \rangle$ plotted as a function of the reaction coordinate d_{react} (in Å) for the hydrogen transfer reaction. The transition state (TS) occurs at $d_{react}=0.95$ Å, where also $\langle s \rangle$ attains its minimum. LSD densities have been employed.

TABLE V. Average values for the reactants, transition states, and products for the two chemical reactions studied. LSD densities were used to calculate all results for the $H+H_2$ and $H+N_2$ reactions, including the difference between the GGA and LSD exchange-correlation energies (in mH).

System	$E_{xc}^{GGA}-E_{xc}^{LSD}$	$\langle r_s\rangle$	$\langle\lvert\zeta\rvert\rangle$	$\langle s\rangle$	R_{xc}^{LSD}	R_{xc}^{GGA}
$H+H_2$	−49.7	1.804	0.549	0.945	0.990	1.001
H_3	−37.7	1.773	0.393	0.870	0.994	0.999
$H+N_2$	−795.0	0.572	0.142	0.754	0.990	1.001
$H+N_2$ (TS)	−781.6	0.570	0.119	0.749	0.991	1.001
HN_2	−776.0	0.567	0.079	0.744	0.992	1.002

GGA; no experimental value is available. As might have been expected from $\langle s\rangle$, the barrier to dissociation of HN_2 is actually lower in GGA (0.39 eV) than in LSD (0.54 eV). Møller-Plesset,[46,47] configuration-interaction calculations,[44] and experiments[46] indicate that HN_2 is metastable with respect to N_2 and H. Our results show that PBE gives a correction in the right direction compared to LSD but predicts HN_2 to be stable by 0.07 eV.

Gradient corrections to energy barriers are most important for processes in which atoms or chemical groups assemble or dis-assemble, including catalysis.[48] In some cases, the transition state may have *fewer* bonds than the initial state. In recent work on barriers to diffusion of Ag adatoms on Ag(100) and Ag(511), Yu and Scheffler[38] compare a variety of LSD and GGA barriers to exchange and hopping diffusion, both on planes and at step edges. In every case the coordination number is reduced at the transition state. Since inhomogeneity effects should outweigh density changes here, Eq. (9) implies that GGA *reduces* barrier heights relative to LSD, consistent with their results. Less severe rearrangements (e.g., internal rotations) may produce little change in $\langle s\rangle$ or $\langle r_s\rangle$ (or in the number of bonds[40]), and thus little difference[40,49,50] between GGA and LSD barriers. For Ag on the much smoother Ag(111) surface, there is only a small difference in LSD and GGA barrier heights.[51]

IV. FINAL REMARKS

We have focussed here on explanations for the effects of gradient corrections, given a particular generalized gradient approximation for $E_{xc}[n_\uparrow,n_\downarrow]$. For qualitative explanations of the physical origins of gradient-corrected nonlocality, see Ref. 52. We stress that accurate density functional approximations need not be empirical; they can be constructed entirely from our current quantitative[8,19,53–55] and qualitative[52] understanding of exchange and correlation. For chemical applications, the most accurate density functionals seem to be those that mix exact exchange[56] with GGA, but even for these the amount of mixing can be constructed nonempirically.[53–55]

Our analysis can be applied to some extent at the exchange-only or Hartree–Fock level, even though LSD and GGA are usually more accurate for exchange and correlation together than for either alone. The GGA enhancement factor for exchange is the $r_s=0$ curve of Fig. 1. It displays a strong nonlocality or s-dependence which tends to underbind molecules (as can be seen from Tables 1 and 2 of Ref. 57) and overestimate energy barriers[42]—the well-known deficiencies of the Hartree–Fock method.

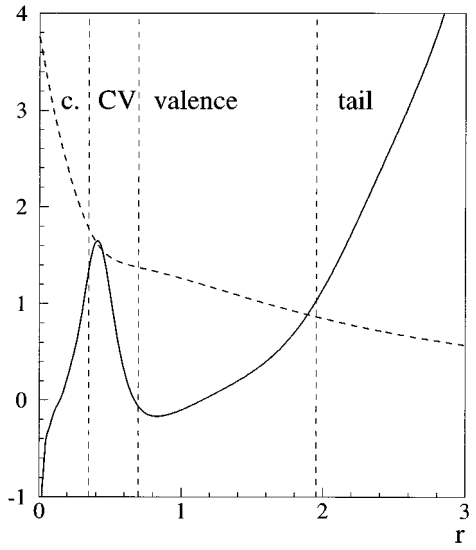

FIG. 9. The reduced Laplacian $\nabla^2 n/(2k_F)^2 n$ (solid curve) for the N atom. The regions marked are those of Fig. 2. Also shown is the dimensionless ratio k_F/k_s (dashed curve), where k_F and k_s are the local Fermi and screening wave vectors.

In Section I, we mentioned another measure of density inhomogeneity, the reduced Laplacian $\nabla^2 n/(2k_F)^2 n$, which is an ingredient of some density functionals.[26,58–60] Figure 9 displays this quantity for the N atom. It is large near the nucleus, in the region of core-valence overlap, and in the tail, but small in the valence region. Also shown in Fig. 9 is the dimensionless ratio k_F/k_s, where $k_s=(4k_F/\pi)^{1/2}$ is the Thomas–Fermi screening wave vector or inverse screening length. This ratio is of some interest because the small parameters of the gradient expansion for the correlation energy are s, $(k_F/k_s)s$, etc.

ACKNOWLEDGMENTS

J.P.P. thanks Peter Feibelman, Jorge Seminario, and Jingsong He for discussions of energy barriers. A.Z. wishes to thank the Slovenian ministry of science and technology for financial support of his Ph.D. studies, and the Tulane physics department, where part of this work was performed. K.B. thanks Nicola Marzari for discussions of surface problems. This work has been supported by National Science Foundation Grant No. DMR95-21353 at Tulane.

[1] R. O. Jones and O. Gunnarsson, Rev. Mod. Phys. **61**, 689 (1989).
[2] R. G. Parr and W. Yang, *Density Functional Theory of Atoms and Molecules* (Oxford, New York, 1989).
[3] R. M. Dreizler and E. K. U. Gross, *Density Functional Theory* (Springer-Verlag, Berlin, 1990).
[4] J. M. Seminario and P. Politzer, Eds., *Modern Density Functional Theory: A Tool for Chemistry* (Elsevier, Amsterdam, 1995).
[5] P. Hohenberg and W. Kohn, Phys. Rev. **136**, B864 (1964).
[6] W. Kohn and L. J. Sham, Phys. Rev. **140**, A1133 (1965).

[7] J. P. Perdew and K. Burke, Int. J. Quantum Chem. **57**, 309 (1996).
[8] J. P. Perdew, K. Burke, and M. Ernzerhof, Phys. Rev. Lett. **77**, 3865 (1996); **78**, 1396(E) (1997). See also Ref. 52.
[9] N. Moll, M. Bockstedte, M. Fuchs, E. Pehlke, and M. Scheffler, Phys. Rev. B **52**, 2550 (1995).
[10] P. H. T. Philipsen and E. J. Baerends, Phys. Rev. B **54**, 5326 (1996).
[11] M. Taut, J. Phys. C **19**, 6009 (1986).
[12] A. Zupan, J. P. Perdew, K. Burke, and M. Causá, Int. J. Quantum Chem. **61**, 835 (1997).
[13] R. Dovesi, C. Pisani, C. Roetti, M. Causà, and V. R. Saunders (unpublished).
[14] R. Dovesi, V. R. Saunders, and C. Roetti (unpublished).
[15] C. Pisani, R. Dovesi, and C. Roetti, *HF Ab Initio Treatment of Crystalline Systems*, Vol. 48 of *Lecture Notes in Chemistry Series* (Springer-Verlag, Berlin, 1988).
[16] M. Towler, A. Zupan, and M. Causà, Comp. Phys. Comm. **98**, 181 (1996).
[17] J. P. Perdew, in *Electronic Structure of Solids '91*, edited by P. Ziesche and H. Eschrig (Akademie Verlag, Berlin, 1991), p. 11.
[18] J. P. Perdew, J. A. Chevary, S. H. Vosko, K. A. Jackson, M. R. Pederson, D. J. Singh, and C. Fiolhais, Phys. Rev. B **46**, 6671 (1992); **48**, 4978 (1993) (E).
[19] J. P. Perdew, K. Burke, and Y. Wang, Phys. Rev. B **54**, 16533 (1996).
[20] Basis sets were obtained from the Extensible Computational Chemistry Environment Basis Set Database, Version 1.0, as developed and distributed by the Molecular Science Computing Facility, Environmental and Molecular Sciences Laboratory which is part of the Pacific Northwest Laboratory, P.O. Box 999, Richland, WA 99352, and funded by the U.S. Department of Energy. The Pacific Northwest Laboratory is a multiprogram laboratory operated by Battelle Memorial Institute for the U.S. Department of Energy under Contract No. DE-AC06-76RLO 1830. Contact David Feller, Karen Schuchardt, or Don Jones for further information.
[21] M. Causà, R. Dovesi, and C. Roetti, Phys. Rev. B **43**, 11937 (1991).
[22] M. Prencipe, A. Zupan, R. Dovesi, E. Aprà, and V. R. Saunders, Phys. Rev. B **51**, 3391 (1995).
[23] W. G. Wyckoff, *Crystal Structures*, 2nd ed. (Wiley, New York, 1963), Vol. 1.
[24] G. Herzberg, *Spectra of Diatomic Molecules* (Van Nostrand-Reinhold, Princeton, NJ, 1970).
[25] A. D. Becke, J. Chem. Phys. **97**, 9173 (1992).
[26] E. I. Proynov, E. Ruiz, A. Vela, and D. R. Salahub, Int. J. Quantum Chem. **S29**, 61 (1995).
[27] B. G. Johnson, P. M. W. Gill, and J. A. Pople, J. Chem. Phys. **98**, 5612 (1993).
[28] V. Ozoliņš and M. Körling, Phys. Rev. B **48**, 18304 (1993).
[29] C. Filippi, D. J. Singh, and C. Umrigar, Phys. Rev. B **50**, 14 947 (1994).
[30] J. C. Grossman, L. Mitas, and K. Raghavachari, Phys. Rev. Lett. **75**, 3870 (1995); **76**, 1006 (1996) (E).
[31] D. R. Hamann, Phys. Rev. Lett. **76**, 660 (1996).
[32] L. Fan and T. Ziegler, J. Chem. Phys. **94**, 6057 (1991).
[33] D. R. Hamann, Phys. Rev. B **55**, R10157 (1997); C. Lee, D. Vanderbilt, K. Laasonen, R. Car, and M. Parrinello, Phys. Rev. Lett. **69**, 462 (1992).
[34] F. Sim, A. St-Amant, I. Papai, and D. R. Salahub, J. Am. Chem. Soc. **114**, 4391 (1992).
[35] D. C. Patton, D. V. Porezag, and M. R. Pederson, Phys. Rev. B **55**, 7454 (1997).
[36] P. Bagno, O. Jepsen, and O. Gunnarsson, Phys. Rev. B **40**, 1997 (1989).
[37] D. J. Singh and J. Ashkenazi, Phys. Rev. B **46**, 11 570 (1992).
[38] B. D. Yu and M. Scheffler, Phys. Rev. Lett. **77**, 1095 (1996).
[39] B. Hammer, K. W. Jacobsen, and J. K. Nørskov, Phys. Rev. Lett. **70**, 3971 (1993).
[40] L. Fan and T. Ziegler, J. Am. Chem. Soc. **114**, 10 890 (1992); L. Deng, T. Ziegler, and L. Fan, J. Chem. Phys. **99**, 3823 (1993).
[41] D. Porezag and M. R. Pederson, J. Chem. Phys. **102**, 9345 (1995).
[42] B. G. Johnson, C. A. Gonzales, P. M. W. Gill, and J. A. Pople, Chem. Phys. Lett. **221**, 100 (1994).
[43] S. P. Walch, R. J. Duchovic, and C. M. Rohlfing, J. Chem. Phys. **90**, 3230 (1989).
[44] S. P. Walch, J. Chem. Phys. **93**, 2384 (1990).
[45] W. R. Schultz and D. J. LeRoy, J. Chem. Phys. **42**, 3869 (1965).
[46] L. A. Curtiss, D. L. Drapcho, and J. A. Pople, Chem. Phys. Lett. **103**, 437 (1984).
[47] S. F. Selgren, P. W. McLoughlin, and G. I. Gellene, J. Chem. Phys. **90**, 1624 (1989).
[48] P. J. Feibelman and J. Harris, Nature **372**, 135 (1994).
[49] J. M. Seminario, M. Grodzicki, and P. Politzer, in *Density Functional Methods in Chemistry*, edited by J. Labanowski and J. Andzelm (Springer, Berlin, 1990).
[50] A. Bormann and R. O. Jones, Chem. Phys. Lett. **252**, 1 (1996).
[51] C. Ratsch, A. P. Seitsonen, and M. Scheffler, Phys. Rev. B **55**, 6750 (1997).
[52] J. P. Perdew, M. Ernzerhof, A. Zupan, and K. Burke (unpublished).
[53] M. Ernzerhof, Chem. Phys. Lett. **263**, 499 (1996).
[54] K. Burke, M. Ernzerhof, and J. P. Perdew, Chem. Phys. Lett. **265**, 115 (1997).
[55] J. P. Perdew, M. Ernzerhof, and K. Burke, J. Chem. Phys. **105**, 9982 (1996).
[56] A. D. Becke, J. Chem. Phys. **98**, 1372 (1993).
[57] M. Ernzerhof, J. P. Perdew, and K. Burke, Int. J. Quantum Chem. (to be published).
[58] J. P. Perdew, Phys. Rev. Lett. **55**, 1665 (1985); **55**, 2370 (1985) (E).
[59] M. Springer, P. S. Svendsen, and U. von Barth, Phys. Rev. B **54**, 17 392 (1996).
[60] Z. Yan, J. P. Perdew, T. Korhonen, and P. Ziesche, Phys. Rev. A (in press).